doi:10.1093/brain/awu298 Brain 2014: 137; 3339–3354 | 3339

BRAIN
A JOURNAL OF NEUROLOGY

White matter involvement in sporadic Creutzfeldt-Jakob disease

Eduardo Caverzasi,[1,2] Maria Luisa Mandelli,[2] Stephen J. DeArmond,[3,4] Christopher P. Hess,[5] Paolo Vitali,[6] Nico Papinutto,[1] Abby Oehler,[3,4] Bruce L. Miller,[2] Irina V. Lobach,[1] Stefano Bastianello,[7] Michael D. Geschwind[2,*] and Roland G. Henry[1,8,9,*]

1 Department of Neurology, University of California San Francisco, San Francisco, CA 94143, USA
2 Memory and Aging Center, Department of Neurology, University of California, San Francisco, CA 94143, USA
3 Department of Pathology, University of California San Francisco, San Francisco, CA 94143, USA
4 Institute for Neurodegenerative Diseases, University of California San Francisco, San Francisco, CA 94143, USA
5 Neuroradiology Division, Department of Radiology & Biomedical Imaging, University of California San Francisco, San Francisco, CA 94143, USA
6 Brain MRI 3T Mondino Research Center, C. Mondino National Neurological Institute, Pavia 27100, Italy
7 Department of Brain and Behavioral Sciences, University of Pavia, Pavia 27100, Italy
8 Bioengineering Graduate Group, University of California San Francisco, San Francisco, CA 94143, USA
9 Department of Radiology and Biomedical Imaging, University of California San Francisco, San Francisco, CA 94143, USA

*These authors contributed equally to this work.

Correspondence to: Eduardo Caverzasi,
Department of Medical Imaging,
3 CC St. Michael's Hospital,
30 Bond Street, Toronto, On,
Canada, M5B 1W8
E-mail: CaverzasiE@smh.ca

Sporadic Creutzfeldt-Jakob disease is considered primarily a disease of grey matter, although the extent of white matter involvement has not been well described. We used diffusion tensor imaging to study the white matter in sporadic Creutzfeldt-Jakob disease compared to healthy control subjects and to correlated magnetic resonance imaging findings with histopathology. Twenty-six patients with sporadic Creutzfeldt-Jakob disease and nine age- and gender-matched healthy control subjects underwent volumetric T_1-weighted and diffusion tensor imaging. Six patients had post-mortem brain analysis available for assessment of neuropathological findings associated with prion disease. Parcellation of the subcortical white matter was performed on 3D T_1-weighted volumes using Freesurfer. Diffusion tensor imaging maps were calculated and transformed to the 3D-T_1 space; the average value for each diffusion metric was calculated in the total white matter and in regional volumes of interest. Tract-based spatial statistics analysis was also performed to investigate the deeper white matter tracts. There was a significant reduction of mean ($P = 0.002$), axial ($P = 0.0003$) and radial ($P = 0.0134$) diffusivities in the total white matter in sporadic Creutzfeldt-Jakob disease. Mean diffusivity was significantly lower in most white matter volumes of interest ($P < 0.05$, corrected for multiple comparisons), with a generally symmetric pattern of involvement in sporadic Creutzfeldt-Jakob disease. Mean diffusivity reduction reflected concomitant decrease of both axial and radial diffusivity, without appreciable changes in white matter anisotropy. Tract-based spatial statistics analysis showed significant reductions of mean diffusivity within the white matter of patients with sporadic Creutzfeldt-Jakob disease, mainly in the left hemisphere, with a strong trend ($P = 0.06$) towards reduced mean diffusivity in most of the white matter bilaterally. In contrast, by visual assessment there was no white matter abnormality either on T_2-weighted or diffusion-weighted images. Widespread reduction in white matter mean diffusivity, however, was apparent visibly on the quantitative attenuation coefficient maps compared to healthy control subjects. Neuropathological analysis showed diffuse astrocytic gliosis and activated microglia in the white matter, rare prion deposition

Received March 14, 2014. Revised August 24, 2014. Accepted August 25, 2014. Advance Access publication November 3, 2014

and subtle subcortical microvacuolization, and patchy foci of demyelination with no evident white matter axonal degeneration. Decreased mean diffusivity on attenuation coefficient maps might be associated with astrocytic gliosis. We show for the first time significant global reduced mean diffusivity within the white matter in sporadic Creutzfeldt-Jakob disease, suggesting possible primary involvement of the white matter, rather than changes secondary to neuronal degeneration/loss.

Keywords: DTI; CJD; mean diffusivity; gliosis; microglia

Abbreviations: CJD = Creutzfeldt-Jakob disease; DTI = diffusion tensor imaging; DWI = diffusion weighted imaging; PrP^{C} = the prion protein; PrP^{Sc} = the prion; TBSS = tract-based spatial statistics; UCSF = University of California of San Francisco

Introduction

Human prion diseases are a group of rare and invariably fatal diseases due to misfolding of the normal protein, the prion protein (PrP^{C}), into an abnormal conformation (the prion or PrP^{Sc}) that causes progressive neurodegeneration in the brain. Sporadic Creutzfeldt-Jakob disease (CJD) is the most common form of human prion disease and classically is characterized by rapidly progressive dementia with ataxia and myoclonus, leading to akinetic mutism and death usually within a year or less from onset (Brown *et al.*, 1986).

MRI has become increasingly important for the clinical diagnosis of sporadic CJD. In addition to its important role in excluding other causes for rapidly progressive dementias, MRI plays an important role in the diagnosis of human prion disease (Geschwind *et al.*, 2009), even early in the illness (Shiga *et al.*, 2004). FLAIR and diffusion weighted imaging (DWI) sequences allow the detection of hyperintensities both within subcortical grey matter (striatum and thalamus) and cortical grey matter (so called 'cortical ribboning') (Young *et al.*, 2005; Satoh *et al.*, 2007; Tschampa *et al.*, 2007; Meissner *et al.*, 2009; Galanaud *et al.*, 2010). DWI hyperintensities in sporadic CJD are more evident and typically positive earlier in the disease than on FLAIR images (Demaerel *et al.*, 1999; Shiga *et al.*, 2004; Vitali *et al.*, 2011). The DWI hyperintensities are due to reduced diffusivity of water molecules in the grey matter, which should be confirmed on mean diffusivity maps (showing hypointensity). Specific neuropathological changes (including vacuolization, prion deposition and possibly astrocytic gliosis) seem to be associated with these grey matter DWI changes (Geschwind *et al.*, 2009). Although sporadic CJD is generally considered to affect primarily grey matter and MRI abnormalities generally have not been observed in white matter, there is histopathological evidence that white matter damage is widespread, with abnormal deposition of neurofilament proteins and neuritic distensions suggesting neuroaxonal pathology (Liberski and Budka, 1999; Armstrong *et al.*, 2002).

Diffusion tensor imaging (DTI) is a non-invasive MRI technique that allows quantitative assessment of microstructural changes in otherwise normal appearing brain tissue. Recently this technique was applied to study 21 patients with E200K genetic prion disease (Lee *et al.*, 2012) and showed reduced fractional anisotropy in many important white matter pathways and suggested that reduced fractional anisotropy was associated with a functional disconnection syndrome (Lee *et al.*, 2012). Whether white matter is primarily affected in CJD or involved secondarily through involvement of cell bodies within the grey matter remains unclear (Kucharczyk and Bergeron, 2004). There are cases of CJD with extensive white matter involvement on T_2-weighted images, which have been referred to as panencephalopathic sporadic CJD. Most reported cases have been in Asia, particularly Japan, and are isolated to patients with long survival due to extensive life-prolonging measures (Mizutani *et al.*, 1981; Kruger *et al.*, 1990; Yamada *et al.*, 1997; Ghorayeb *et al.*, 1998; Matsusue *et al.*, 2004; Hama *et al.*, 2009). White matter abnormalities in these patients might simply be the result of secondary Wallerian degeneration and not related to primary involvement of the white matter (Jansen *et al.*, 2009; Deguchi *et al.*, 2012). A recent paper focusing on DTI measures (fractional anisotropy, mean diffusivity, axial diffusivity, and radial diffusivity) in the caudate, corpus callosum, posterior limb of the internal capsule, pulvinar, precuneus, and frontal lobe, found no significant white matter abnormalities in a small sporadic CJD group compared to healthy subjects or a cohort of subjects with rapidly progressive dementia (Wang *et al.*, 2013). To our knowledge, however, no studies to date have addressed how DTI parameters change across the entire brain within the white matter of patients with sporadic CJD. The aims of this study were: (i) to determine quantitatively whether white matter diffusion changes occur in sporadic CJD; (ii) to describe the pattern of white matter involvement using quantitative diffusion and visual assessment; and (iii) to correlate white matter histopathology with the MRI changes.

Materials and methods

This study was approved by the University of California of San Francisco (UCSF) Committee on Human Research.

Subjects

Subjects enrolled for this study were evaluated between August 2005 and August 2008 at the UCSF Memory and Ageing Centre. Of 61 serial probable or definite sporadic CJD patients evaluated during this period, 31 underwent the same MRI protocol and 26 with adequate quality MRI for post-processing were included in this study. Twenty-three of the subjects with sporadic CJD (88%) had definite CJD and three were not pathology proven, but eventually met UCSF 2007 probable sporadic CJD criteria (Geschwind *et al.*, 2007) and either WHO 1998 or European probable sporadic CJD criteria (Zerr *et al.*, 2009). Control MRIs were obtained from the same scanner on nine age and gender-matched healthy subjects (Table 1). Seven subjects with sporadic CJD had a second serial brain MRI after ~2 months

[2.17, standard deviation (SD) ± 0.23 months] (Caverzasi *et al.*, 2014). All subjects with sporadic CJD had the Mini-Mental State Examination, modified Barthel Index (Mahoney and Barthel, 1965), Neuropsychiatric Inventory Scale (to assess behavioural impairments) (Cummings, 1997), and a detailed standardized neurological examination (± 3 days to the MRI scan date) (Table 1 and Supplementary material).

Neuropathology

Sporadic CJD brain autopsies were performed at UCSF ($n = 19$) and/or the National Prion Disease Pathology Surveillance Centre (NPDPSC; $n = 4$) (Kretzschmar *et al.*, 1996). Detailed brain specimens used for MRI-pathology white matter comparison were obtained for six subjects with sporadic CJD autopsied at UCSF for whom tissue was still available.

MRI acquisition

Images were acquired on a 1.5 T GE Signa scanner. The acquisition protocol consisted of a T_1-weighted 3D IRSPGR (inversion recovery spoiled gradient) axial slab with 60 slices of 3 mm thickness, repetition/echo times = 27/6 ms, flip angle 40°, in-plane matrix 256 × 256 covering a field of view of 24 × 24 cm^2), an axial T_2 FLAIR (48 slices of 3 mm thickness, repetition/echo/inversion times = 8802/122/2200 ms, 512 × 512 matrix with a field of view of 24 × 24 cm^2), and a DTI axial acquisition (15 non-collinear gradient directions with b = 1000 s/mm^2, one b = 0 reference image, 35 contiguous slices of 3 mm thickness, repetition/echo times = 12 400/69 ms, 128 × 128 matrix covering a field of view of 25.6 × 25.6 cm^2 interpolated to give a final 1 × 1 × 3 mm^3 resolution).

Imaging processing

To investigate the involvement of the white matter in sporadic CJD both cross-sectionally and longitudinally, we performed a volume of interest analysis in each subject's native DTI space after automated parcellation of T_1 volumes using Freesurfer Image Analysis Suite Version 4.5. Voxel-based analysis was also performed in a common standard space using the Tract-Based Spatial Statistics (TBSS) methods implemented in FSL (FMRIB, Oxford UK, http://www.fmrib.ox.ac.uk/fsl) (Smith *et al.*, 2006).

Volume of interest analysis

Automated parcellation of T_1 images. Masks of whole brain grey and white matter were extracted and the Desikan-Killiany Atlas in Freesurfer was used to obtain 34 grey matter volumes of interest per hemisphere in the native coordinate system of each subject (Dale *et al.*, 1999; Fischl *et al.*, 1999). Subcortical white matter boundaries were defined from the grey matter parcellations by defining outer boundaries 4 mm subjacent to each cortical region. Thus each subcortical white matter volume of interest included the area of white matter 4 mm below the grey-white border for each Freesurfer parcel. Accuracy of the segmentation results was validated by a neuroradiologist (E.C.) and was reprocessed until correct or if it failed to adequately segment it was excluded.

DTI processing. After correcting for distortions due to eddy current and head motion, maps of fractional anisotropy, mean diffusivity, axial diffusivity and radial diffusivity were calculated by fitting the diffusion tensor model within each voxel using the FDT software tool in FSL. To improve the visualization of white matter difference in mean diffusivity maps we also created 'attenuation coefficient maps' [attenuation coefficient = $\exp^{(-b \times \text{mean diffusivity})}$]. In these images, typical diffusion contrast is inverted and differences enhanced. B = 0 images were then registered to the brain-extracted volumes from T_1-weighted images using an affine alignment (FLIRT). The transformation matrix obtained was then applied to the DTI parameter maps. The mean values for mean diffusivity, fractional anisotropy, axial and radial diffusivity were calculated in the total white matter and within each volume of interest on co-registered images.

Statistical analysis. For cross-sectional comparisons, the non-parametric Wilcoxon test was applied to age-corrected Z-scores to evaluate differences of mean diffusivity, fractional anisotropy, axial and radial diffusivity values in the total white matter and in each

Table 1 Demographics of the healthy control and sporadic CJD cohort[a]

Group	*n*	Sex	Age	Time between symptoms outbreak and MRI (months)	Total disease duration (months)	% Path-proven	Codon 129[b]	Molecular classification	
Healthy controls	9	4F (44%); 5M (56%)	61 ± 16	—	—	—	—	—	
Sporadic CJD	26	12F (46%); 14M (54%)	62 ± 9	12 ± 8	19 ± 13	88%	MM 58%[c]	MM 1	15%
								MM 2	23%
								MM 1/2	12%
								MM N/A	8%
							MV 31%	MV1	8%
								MV2	15%
								MV 1/2	4%
								MV N/A	4%
							VV 8%	VV 2	8%
							N/A 4%	N/A	4%

[a]See text for demographics on controls subjects.
[b]All but one subject with sporadic CJD ruled out for genetic prion disease by PRNP analysis; this subject was not path-proven, but had no family history of neuropsychiatric disorder and presented clinically like sporadic CJD.
[c]One subject with codon 129 data, but no prion typing on western blot available, was called MM 1 based on the histopathology autopsy findings. Percentages might not add exactly due to rounding.
— = not relevant; N/A = data not available; M = methionine; V = valine. ± refers to standard deviation (SD). Previously published and used with permission (Caverzasi *et al.*, 2014).

subcortical white matter volume of interest. The non-parametric Wilcoxon signed rank test was used to evaluate differences between the first and second MRI time points. False discovery rate (FDR) with $P < 0.05$ was used to correct for multiple comparisons.

Tract-based spatial statistics analysis

Voxel-wise TBSS analysis was performed using the default parameters in the FSL (Smith *et al.*, 2006). Specifically, fractional anisotropy maps for each subject were normalized to the FMRIB58 fractional anisotropy template in the Montreal Neurological Institute (MNI) standard space using both linear (FLIRT) and non-linear (FNIRT) registration. A mean fractional anisotropy image was created and thinned to create a mean fractional anisotropy skeleton, which represents the centres of all tracts common to the group. Each subject's aligned fractional anisotropy, mean, axial and radial diffusivity data were then projected onto this skeleton, allowing voxel-wise between-group comparisons. Comparisons of mean diffusivity, fractional anisotropy, axial and radial diffusivity were tested by using a two-sample *t*-test adjusting for the subject's age. The number of permutations was set at 5000. The resulting statistical maps were corrected for multiple comparisons [family-wise error (FWE) correction using the threshold-free cluster enhancement option] and thresholded at $P = 0.05$. Results were also assessed at uncorrected statistical $P = 0.05$ in order to visually assess statistical trends. The anatomical location of significant clusters was detected using the Johns Hopkins University white matter tractography atlas and the International Consortium of Brain Mapping ICBM–DTI white matter labels atlas. The number of voxels that were significantly different in patients compared to control subjects was reported for each white matter tract. To understand the relative contribution of axial and radial diffusivity to either mean diffusivity or fractional anisotropy changes, we performed an additional region of interest-based analysis, selecting clusters of voxels with either significant mean diffusivity or fractional anisotropy reduction (Lee *et al.*, 2012); to increase the likelihood of identifying voxels with mean diffusivity or fractional anisotropy changes and to identify strong trends, we selected voxels with a $P < 0.06$ (FDR corrected). Average mean diffusivity, fractional anisotropy, axial and radial diffusivity were derived in these clusters. The non-parametric Wilcoxon signed rank test was used to evaluate differences between sporadic CJD and controls in these selected regions.

MRI white matter visual assessment

To determine the effect of any T_2-weighted abnormalities on DTI metric results, two radiologists (E.C., C.H.) independently reviewed T_2-weighted images from the first scan of the 26 patients with sporadic CJD and rated any white matter abnormalities based on the modified scale developed by Scheltens *et al*. (1993) (periventricular white matter score 0–6, deep white matter score 0–24; total score: 0–30) (Scheltens *et al.*, 1993; Pantoni *et al.*, 2002). Differences were resolved by consensus. In each subject in whom areas of T_2-weighted white matter abnormalities were noted, we compared the DTI metrics maps in these areas with their normal appearing white matter.

Histopathology evaluation

Sufficient samples of white matter still were available on six of the 19 autopsied subjects. In five of six patients white matter samples were taken from the middle-superior frontal, inferior parietal and internal capsule regions. For Subject 12 parietal tissue was not available, so a superior temporal tissue block was used. The subcortical samples were ~1 cm^3 blocks and included subcortical white matter with overlying grey matter and portion of deeper white matter. The internal capsule samples included a portion of the thalamus.

Formalin-fixed samples were processed, paraffin-embedded, and sectioned at 8 μm thickness. The sections were stained with haematoxylin and eosin (Fisher Scientific cat# SH26-500D and cat# 245-658) or processed for immunohistochemistry with the PrP-specific 3F4 monoclonal antibody (Prusiner Laboratory, UCSF) and for astrocytes with an anti-GFAP antibody (Dako cat# Z0334). Secondary antibodies used for 3F4 and GFAP were a biotinylated horse anti-mouse IgG antibody (Vector laboratories cat# BA-2000) and a biotinylated goat anti-rabbit IgG antibody (Vector laboratories cat# BA-1000), respectively. The peroxidase substrate DAB kit (Vector laboratories cat# SK-4100) was used for colour development. Bielschowsky silver stain was used to evaluate white matter axonal degeneration.

A neuropathologist (S.J.D.) with extensive experience in CJD pathology assessed the severity and extent of histopathological changes in each white matter region comparing with the overlying grey matter. The degree of astrocytic gliosis and prion deposition was graded according to a 4-point scale (0, absent; 1, mild; 2, moderate; 3, severe) and by the percentage of each area involved. For vacuolization, only the percentage of area involved was assessed. The Spearman non-parametric test was used to assess the correlation between histopathology rating results and the quantitative metrics results, as well as with visual assessment rating scores in the frontal and parietal lobes. For correlation of quantified MRI data with neuropathology, we used the last UCSF MRI; two of the six subjects (Subjects 2 and 5) with neuropathology had serial MRIs, and we used their second/last UCSF MRI. The MRI data used for the analysis comparing MRI (visual assessment and mean diffusivity) to pathological findings were acquired over a mean 81 ± SD 79 days before death (range 9–205; median 67.5 days). After the initial histopathological analysis, to identify any activated microglia associated with reactive astrocytosis or areas of demyelination, we reanalysed and processed the tissue with immunohistochemistry with anti-IBA1 antibody (Wako #019-19741) (Kanazawa *et al.*, 2002) and with Luxol Fast blue or Cresyl violet, respectively.

Results

Total white matter and subcortical white matter analyses

In the total white matter volume, there was a significant reduction in the average mean diffusivity [healthy controls = 0.817×10^{-3} mm^2/s (±0.041 SD), sporadic CJD = 0.749 (±0.055); $P = 0.002$], axial diffusivity [healthy controls = 1.143 (±0.077), sporadic CJD = 1.031 (±0.065); $P = 0.0003$] and radial diffusivity [healthy controls = 0.654 (±0.026), sporadic CJD = 0.608 (±0.054); $P = 0.013$] in sporadic CJD subjects compared to controls. There was a trend towards reduced fractional anisotropy in the total white matter [healthy controls = 0.356 (±0.023), sporadic CJD = 0.337 (±0.033), $P = 0.06$].

Regional analyses of subcortical white matter showed mean diffusivity was significantly reduced in the majority of subcortical white matter volumes of interest (Table 2 and Fig. 1); no increase in mean diffusivity was observed in any volumes of interest. The group-wise pattern of involvement was relatively symmetric,

Table 2 Cross-sectional analysis of DTI metrics in the subcortical white matter volumes of interest in patients with sporadic CJD compared with control subjects after multi-comparison correction (FDR)

Subcortical white matter volumes of interest		MD		FA		AD		RD	
		Left	Right	Left	Right	Left	Right	Left	Right
Frontal	**Control**	840 ± 70	836 ± 61	0.318 ± 0.024	0.314 ± 0.025	1105 ± 87	1104 ± 87	687 ± 47	691 ± 49
	sporadic CJD	757 ± 64	751 ± 69	0.303 ± 0.037	0.303 ± 0.04	998 ± 70	993 ± 79	637 ± 64	633 ± 68
Caudal middle-frontal		**	**	NS	NS	**	*	*	*
Lateral orbito-frontal		**	**	NS	(*)	**	**	(*)	(*)
Medial orbito-frontal		*	**	NS	*	**	**	NS	(*)
Pars opercularis		**	**	NS	NS	**	**	*	*
Paracentral		**	*	NS	NS	**	*	(*)	NS
Pars orbitalis		**	*	NS	NS	**	**	*	(*)
Pars triangularis		*	**	NS	NS	**	**	(*)	*
Precentral		**	**	NS	NS	**	*	(*)	*
Rostral middle frontal		**	**	NS	NS	**	**	*	*
Superior frontal		**	**	NS	NS	**	**	(*)	(*)
Frontal pole		NS	NS	NS	NS	NS	NS	NS	NS
	Control	859 ± 62	873 ± 66	0.403 ± 0.029	0.397 ± 0.033	1249 ± 93	1270 ± 116	652 ± 48	666 ± 45
Limbic	**sporadic CJD**	789 ± 62	794 ± 65	0.372 ± 0.043	0.368 ± 0.044	1123 ± 73	1126 ± 83	622 ± 64	628 ± 81
Caudal anterior cingulate		(*)	(*)	(*)	*	**	**	NS	NS
Isthmus cingulate		**	**	NS	NS	**	**	(*)	*
Posterior cingulate		*	*	*	*	**	**	NS	NS
Rostral anterior cingulate		**	**	NS	**	**	***	(*)	NS
Insula		**	**	(*)	NS	**	**	NS	(*)
	Control	855 ± 59	838 ± 58	0.307 ± 0.031	0.300 ± 0.022	1129 ± 79	1105 ± 81	710 ± 49	703 ± 48
Temporal	**sporadic CJD**	757 ± 75	739 ± 75	0.288 ± 0.033	0.282 ± 0.036	991 ± 87	963 ± 91	642 ± 72	632 ± 71
Entorhinal		**	*	(*)	(*)	**	**	(*)	(*)
Fusiform		*	*	NS	NS	**	*	(*)	(*)
Inferior temporal		**	**	NS	NS	**	**	*	**
Middle temporal		**	**	NS	NS	**	**	*	*
Temporal pole		*	NS	NS	*	(*)	*	NS	NS
Parahippocampal		**	**	*	NS	***	**	*	*
Superior-temporal		**	**	NS	NS	**	**	*	*
Transverse temporal		**	(*)	NS	NS	*	(*)	*	NS
Banks superior temporal sulcus		**	**	NS	NS	**	**	*	**
	Control	828 ± 60	818 ± 57	0.314 ± 0.028	0.314 ± 0.031	1092 ± 74	1077 ± 75	681 ± 42	673 ± 39
Parietal	**sporadic CJD**	730 ± 72	725 ± 71	0.313 ± 0.035	0.313 ± 0.037	974 ± 83	968 ± 81	608 ± 70	605 ± 69
Inferior parietal		**	**	NS	NS	**	**	*	**
Postcentral		**	**	NS	NS	**	*	**	*
Precuneus		**	**	NS	NS	**	**	**	**
Superior parietal		**	*	NS	NS	**	*	*	*
Supramarginal		**	**	NS	NS	**	**	*	*
	Control	832 ± 37	823 ± 42	0.276 ± 0.032	0.279 ± 0.036	1073 ± 58	1062 ± 62	711 ± 35	701 ± 36
Occipital	**sporadic CJD**	742 ± 83	729 ± 84	0.258 ± 0.039	0.265 ± 0.038	948 ± 94	936 ± 99	642 ± 80	628 ± 81
Cuneus		**	**	NS	NS	**	**	*	*
Lateral occipital		*	*	NS	NS	**	**	(*)	*
Lingual		**	**	NS	NS	**	**	*	*
Pericalcarine		**	**	NS	NS	**	**	**	*

Mean diffusivity, axial and radial diffusivity values are reported in $mm^2/s \times 10^{-3}$ at a lobar level as average ± SD for both control and sporadic CJD groups. The significance is reported as $***P < 0.001$, $**P < 0.01$, $*P < 0.05$, (*) trend with $P < 0.1$, with sporadic CJD DTI metrics reduced versus controls. NS = non-significant; MD = mean diffusivity; FA = fractional anisotropy; AD = axial diffusivity; RD = radial diffusivity. No DTI metrics were increased in any volumes of interest in sporadic CJD.

except some temporal lobe regions in which the left hemisphere was more involved than the right hemisphere (Table 2 and Supplementary Table 1).

Most volumes of interest had no changes in fractional anisotropy, although a few showed a significant (or trend towards) reduction in fractional anisotropy (Fig. 1, Table 2 and Supplementary Table 1). Similar to mean diffusivity, axial diffusivity was significantly reduced in the subjects with sporadic CJD compared to controls in all but two volumes of interest, in which there was a trend towards reduction (Table 2 and Supplementary Table 1); the patterns of reduced axial and mean diffusivity were almost identical. Radial diffusivity was reduced in almost all temporal, parietal

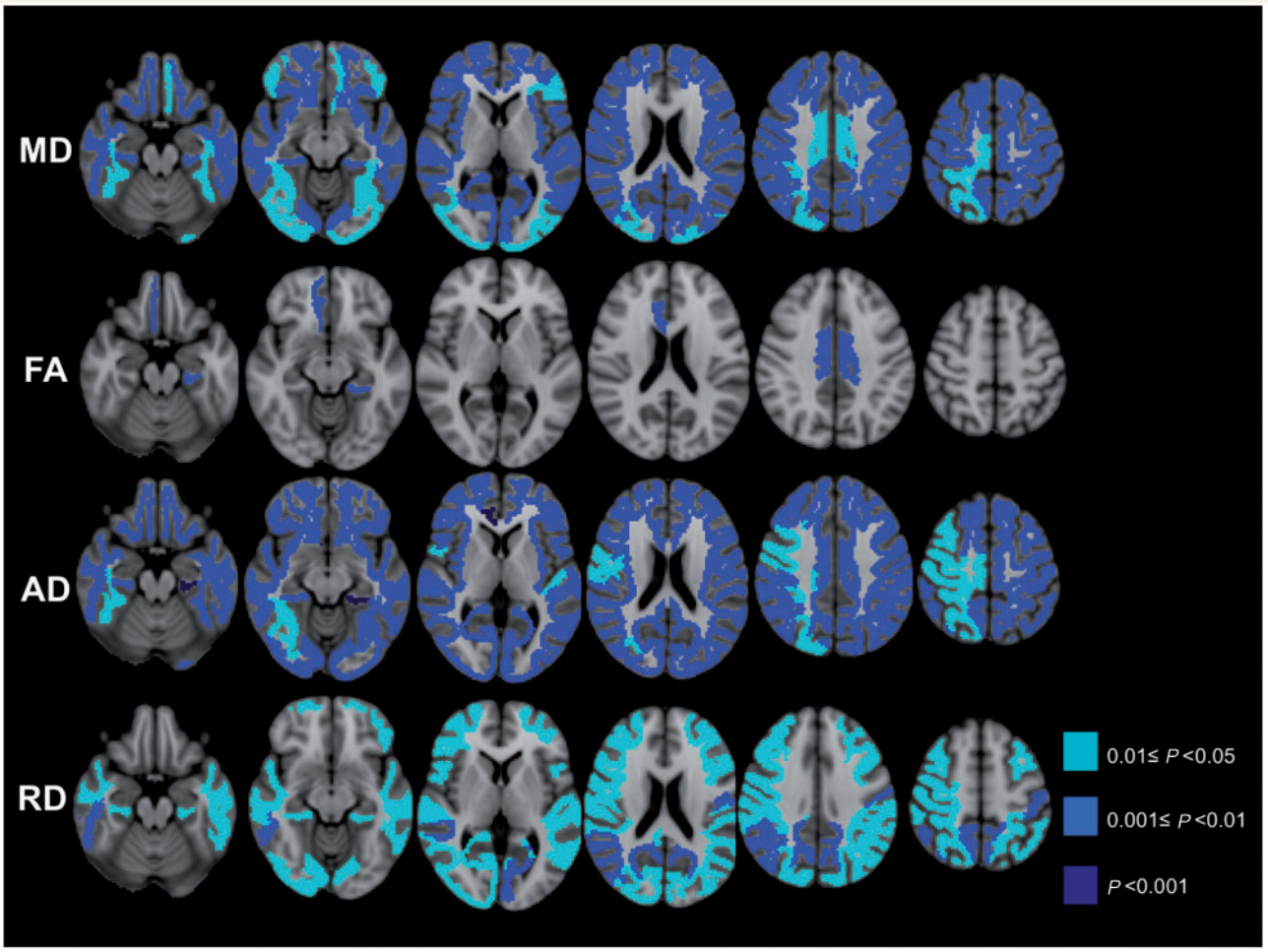

Figure 1 Cross-sectional subcortical white matter analysis DTI metrics results. Subcortical white matter volumes of interest analysis results. Figure shows volumes of interest with either significant reduced mean diffusivity (MD), fractional anisotropy (FA), axial diffusivity (AD) and/or radial diffusivity (RD) in sporadic CJD compared with controls after correction for multiple comparisons (FDR). Colour-scale shows *P*-values of significance. Orientation is radiologic (right brain is left side of image). There were no subcortical white matter volumes of interest showing significantly increased DTI metrics in sporadic CJD versus controls after correction for multiple comparisons (FDR).

and occipital white matter volumes of interest, but less widely in the frontal, limbic white matter volumes of interest, although there was a trend towards reduction in these regions (Table 2 and Supplementary Table 1). Therefore, mean diffusivity reduction seems due to a concomitant reduction of both axial diffusivity and radial diffusivity, without appreciable changes in white matter anisotropy (fractional anisotropy overall was relatively normal). There was a statistically significant positive correlation (Spearman's $\rho = 0.64$, $P < 0.001$) between the subcortical white matter mean diffusivity and the overlying cortical grey matter mean diffusivity values, which we had calculated previously in the same subjects (Caverzasi *et al.*, 2014). In the subgroup of seven patients with serial MRIs, there were no significant differences in DTI metrics differences between first and second MRI time points, either within the total white matter or within the volume of interest-based subcortical white matter analysis.

Tract-based spatial statistics analysis

Mean diffusivity was significantly reduced in subjects with sporadic CJD compared to controls in the left hemisphere involving both the anterior and posterior limbs of the internal capsule, the corticospinal tract, the inferior fronto-occipital fasciculus and the uncinate fasciculus ($P < 0.05$, FWE) (Fig. 2). There was, however, a more widespread trend ($0.05 < P < 0.1$, FWE) towards reduced mean diffusivity in the homologous regions of the right hemisphere and bilaterally in the anterior thalamic radiations, the left inferior superior longitudinal fascicles and the left fornix (not shown).

Fractional anisotropy was significantly reduced in subjects with sporadic CJD compared to controls bilaterally in only a few regions: the anterior limbs of the internal capsule, the anterior portion of the external/extreme capsule, the fornix, the genu of the corpus callosum, the rostral portion of the inferior fronto-occipital fasciculus, and the uncinate fasciculus ($P < 0.05$, FWE) (Fig. 2).

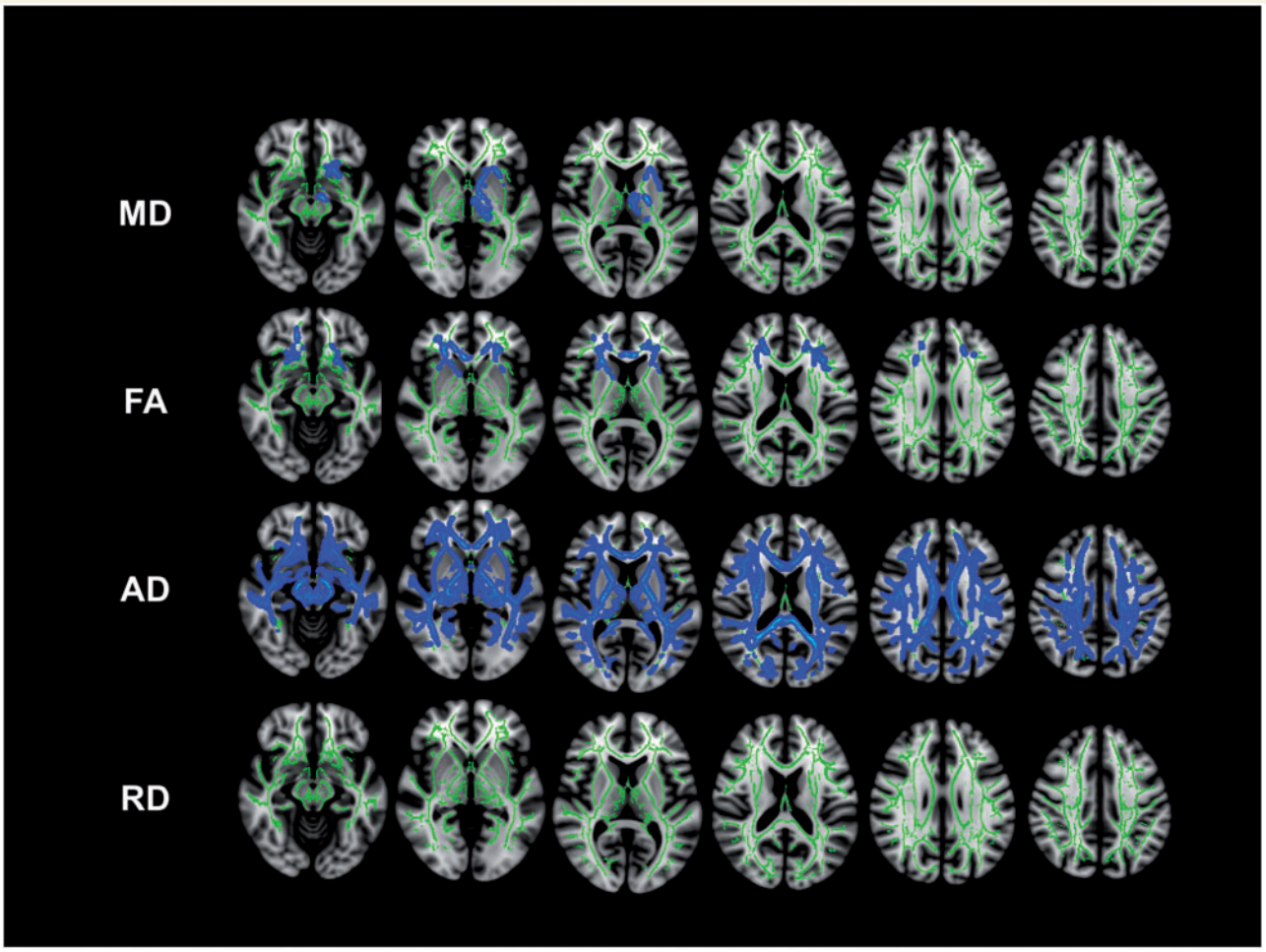

Figure 2 TBSS cross-sectional group-wise analysis of sporadic CJD versus controls. Significant areas (blue code) of decreased DTI metrics in sporadic CJD versus controls are shown in the skeleton (green) ($P < 0.05$). There was a statistically significant reduction of mean diffusivity (MD) in the left hemisphere in the limbs of the internal capsule, the thalamic radiations, inferior fronto-occipital fasciculus and uncinate fasciculus. There was a significant reduction of fractional anisotropy (FA) bilaterally in the frontal lobe. There was a statistically significant reduction of axial diffusivity (AD) in the majority of white matter, whereas no areas of reduced radial diffusivity (RD). None of the DTI metrics showed increased values in sporadic CJD compared to controls ($P < 0.05$). By slightly lowering the threshold for significance to $P \leqslant 0.06$, many more regions in multiple areas of the TBBS skeleton showed decreased average mean diffusivity (Supplementary material). TBSS white matter skeleton of the occipital lobes is not shown, due to the lack of any statistically significant DTI metric changes in this region.

In contrast, axial diffusivity was widely reduced in almost all TBSS skeleton regions ($P < 0.05$, FWE) (Fig. 2). Although there were no statistically significant changes in radial diffusivity, there was a trend towards reduction ($0.05 < P < 0.1$, FWE) in most TBSS skeleton regions (Fig. 2). To better understand the contribution of DTI metrics to the diffusion changes, we performed a region of interest-based analysis, selecting clusters of voxels with either significant mean diffusivity or fractional anisotropy reduction in sporadic CJD compared to controls (Lee *et al.*, 2012); this analysis showed that: (i) in regions with reduced mean diffusivity, the decreased mean diffusivity seemed to be due to a similar contribution from both reduced axial and radial diffusivity (Supplementary Fig. 1A), leading to a fractional anisotropy within normal range; and (ii) in regions with reduced fractional anisotropy, the decreased fractional anisotropy seemed to be due to significantly reduced axial diffusivity, whereas the radial diffusivity was normal (Supplementary Fig. 1B). These findings are concordant with the Freesurfer analysis.

Histopathology

In one of six sporadic CJD cases reviewed for white matter pathology (subject 5), there was mild to moderate PrP^{Sc} staining in the subcortical and deep white matter of both hemispheres (Fig. 3J and Table 3); the white matter PrP^{Sc} staining was less intense, however, than in the overlying cerebral cortex (Fig. 3I and J). White matter of the remaining five sporadic CJD cases had little or no PrP^{Sc} staining in either the subcortical or deep white matter (Fig. 3D), particularly when compared to the overlying cortical grey matter (Fig. 3C). The other abnormality found in subject 5

Table 3 White matter histopathology ratings in three brain regions in six subjects with sporadic CJD with available pathology

Sporadic CJD subject ID	MRI to death interval (days)	Frontal lobe			Parietal lobe			Internal capsule		
		PrP^{Sc} severity: % area	Gliosis severity: % area	Vacuolation % area	PrP^{Sc} severity: % area	Gliosis severity: % area	Vacuolation % area	PrP^{Sc} severity: % area	Gliosis severity: % area	Vacuolation% area
2	205 #	0.5: 100% (fine)	0.5: 80% 2: 20%	<5%	0.5: 100%	1: 80% 2: 20%	<5%	0: 100%	2: 100%	<5%
5	123 #	0: 75% 1: 25% (fine and course)	2: 80% 3: 20%	<5%	0: 30% 1: 70% (fine and course)	1: 30% 2: 60% 3: 10%	<5%	0: 95% 1: 5%	2: 100%	<5%
12*	14	0: 100%	2: 40% 3: 60%	<5%	0%	1: 40% 2: 60%	<5%	0: 100%	2.5: 100%	<5%
13	114	0: 100%	2 × 50% 3 × 50%	<5%	0.5 × 100%	1: 25% 2: 25% 3: 50%	<5%	0: 100%	1: 100%	<5%
18	9	0: 90% 1: 10% (fine)	2: 30% 3: 70%	<5%	0: 100%	1.5: 30% 2.5: 70%	<5%	0: 100%	2: 100%	<5%
26	21	0: 100%	1: 70% 2: 30%	<5%	0%	0: 60% 1: 30% 2: 10%	<5%	0: 100%	2: 100%	<5%

Subjects are listed based on the time interval between MRI and death. PrP^{Sc} deposition, gliosis and vacuolation are reported as % of area involved. For gliosis and PrP^{Sc} deposition a rate of involvement was performed (0 = none; 1 = mild; 2 = moderate; 3 = severe). Scores in between two ordinals were graded with '0.5'; PrP^{Sc} deposition was also described as fine or course. Subjects 5 was the single case considered to have PrP^{Sc} in the white matter.
* Subject 12, as parietal tissue was not available for all immunohistochemistry, superior temporal was used instead.
# Second time point MRI.

was moderately intense and diffuse reactive astrocytic gliosis (Fig. 3L and Table 3); the same degree of reactive astrocytic gliosis, however, was found in the white matter of all other sporadic CJD cases and thus did not necessarily co-localize with PrP^{Sc} (Fig. 3F). Reactive astrocytic gliosis of the cerebral cortex was significantly more intense in the white matter than in the grey matter (Fig. 3E and F), with an increased number of reactive astrocytes, which had more staining of processes (filled with GFAP immunopositive fibrils) and enlarged cell bodies (Fig. 4A and D) in all cases. In the grey matter of the cerebral cortex, there was a moderate, patchy reactive astrocytosis (although mild relative to the reactive astrocytosis in the white matter) and generally confined to layers 1 (Fig. 3E and K) and 6 (not shown). Areas of cortical grey matter with reactive astrocytosis seemed to accompany PrP^{Sc} deposition (Fig. 3C, E, I and K). Most of the intense reactive astrocytes appeared to surround arterioles. In areas without PrP^{Sc}, there was no reactive astrocytic gliosis (not shown). Finally, standard vacuolation, as typically seen in grey matter in sporadic CJD, was seen in only ~5% of white matter in all subjects, regardless of the presence of PrP^{Sc} (Fig. 3B and H). Occasional micro 'vacuoles' were found focally in the white matter of the sporadic CJD cases with PrP^{Sc} (not shown); these were considered artefacts, however, as they were not like the typical vacuolation of grey matter seen in prion disease and because they can be found in non-CJD cases. Typical vacuoles in the grey matter (Figs. 3A and G) were found in synaptic regions in all cases. In all patients there were patchy foci of white matter demyelination in all regions evaluated. No evident axonal degeneration in the white matter was present in any of the cases.

In all cases activated microglia were found throughout the grey matter (Fig. 4B) and white matter (Fig. 4E). In both the grey matter and white matter, activated microglia often seemed intimately associated with reactive astrocytes (Fig. 4C and F); in the white matter, however, activated microglia were primarily found associated with reactive astrocytes (Fig. 4F), whereas in the grey matter, activated microglia were in all regions regardless of the amount of reactive astrocytosis (*cf.* Fig. 4A and B with Fig. 4D and E). There was not a statistically significant correlation between histopathological rating scores and any DTI metrics (Spearman's $P > 0.1$), including mean diffusivity values (PrP^{Sc} deposition: Spearman's $\rho = -0.26$, $P = 0.41$; gliosis: Spearman's $\rho = 0.21$, $P = 0.5$; vacuolation: Spearman's $\rho = 0.1$, $P = 0.75$). Even when we excluded Subject 2, an outlier with by far the longest MRI to death interval, there were still no correlations.

MRI visual assessment of white matter

Regarding the concordance of the two readers conducting the MRI white matter visual assessment, the mean inter-rater precise agreement for each modified Scheltens score for all regions was 81 ± 6%. Concordance of modified Scheltens scores for total brain white matter (mild, moderate, severe), however, was 100%. The mean average modified Scheltens score of white matter hyperintensities was 5.3 of 30 (±4 SD), within the mild range. Eighty-eight per cent of subjects had mild white matter involvement (modified Scheltens score 0–10), 12% showed moderate involvement (scores 11–20) and none showed severe white matter involvement. Side-by-side comparison of the visually rated white matter abnormalities with the mean diffusivity maps showed that all regions with white matter abnormalities seemed as normal to increased (none with decreased) mean diffusivity (Supplementary Fig. 2). Comparing the white matter histopathological findings (Table 3) to white matter abnormalities by visual

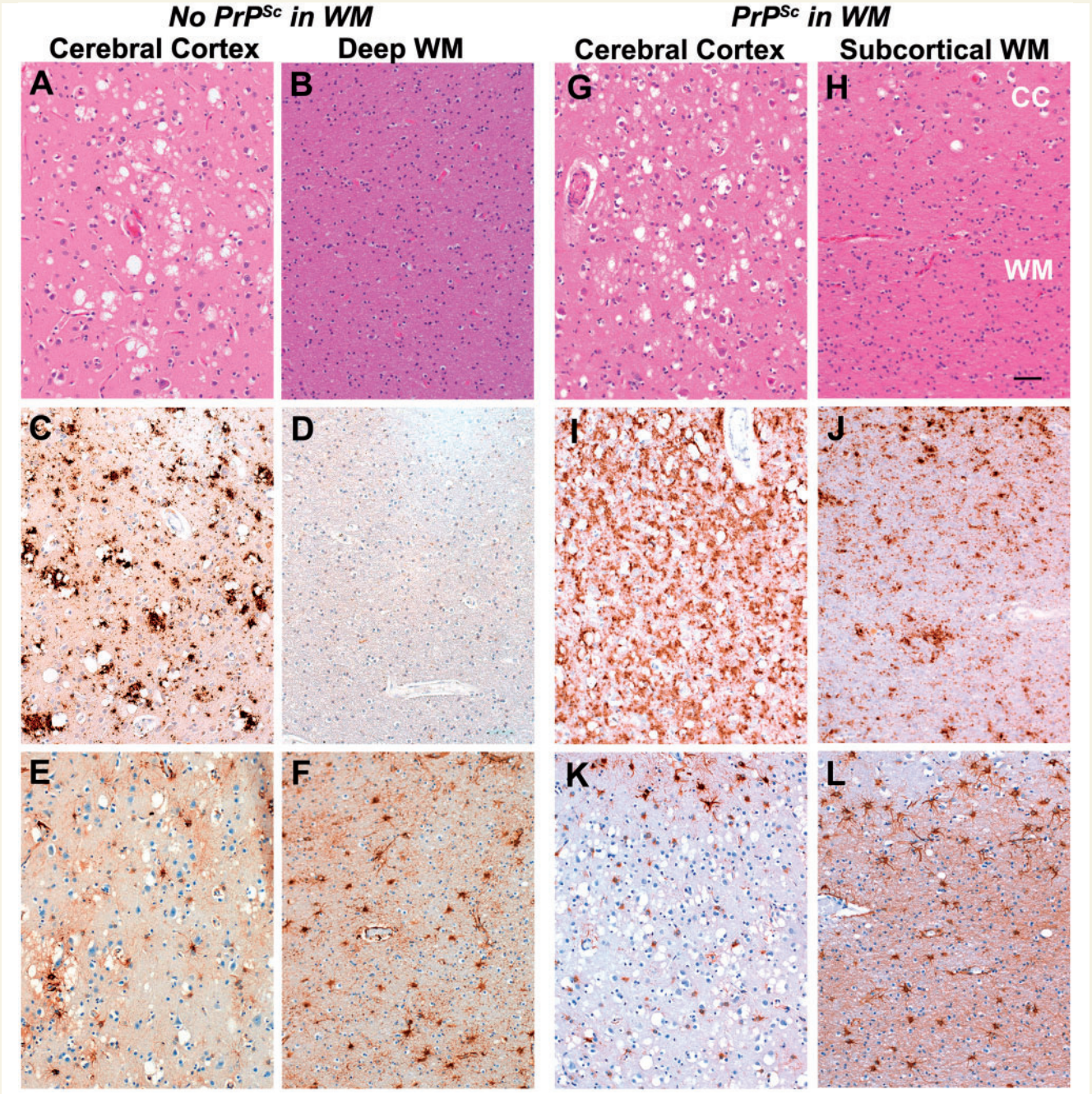

Figure 3 Histopathology findings. Examples of the main neuropathological changes found in sporadic CJD cases without white matter PrP^{Sc} (**A–F**, Subject 18, see Table 3) and with mild white matter PrP^{Sc} (**G–L**) (Subject 5 in Table 3) (**A**, **B**, **G** and **H**) Haematoxylin and eosin stain showing vacuolation. The 3F4 immunohistochemistry stain (**C**, **D**, **I** and J) shows finely granular and coarse Pri^{Sca} deposition throughout the cerebral cortex in the case without white matter staining (**C**) and diffuse granular staining throughout the cortex in the case with white matter PrP^{Sc} (**I**). No PrP^{Sc} is found in the deep cerebral white matter (**D**). PrP^{Sc} is seen in layer 6 of the cerebral cortex (CC, upper 20% of **J**) and in the subcortical (lower 80% of **J**) and deep white matter (not shown). Anti-GFAP antibody immunohistochemistry stain (**E**, **F**, **K** and **L**) shows more intense reactive astrocytic gliosis in the white matter (**F** and **L**) than in the cerebral cortex (**E** and **K**: panels show only layers 1 to 3). Scale bar: **H** = 100 μm, and applies to all panels. WM = white matter; CC = cerebral cortex grey matter.

assessment (Supplementary Table 2) in the frontal and parietal lobes, there were no statistically significant correlations, in particular between Scheltens rating scores and gliosis (Spearman's $\rho = 0.43$, P value = 0.16).

To identify possible changes in the normal appearing white matter (on FLAIR images) we created attenuation coefficient maps. Interestingly, all sporadic CJD attenuation coefficient maps showed widespread clearly visible reduced mean diffusivity

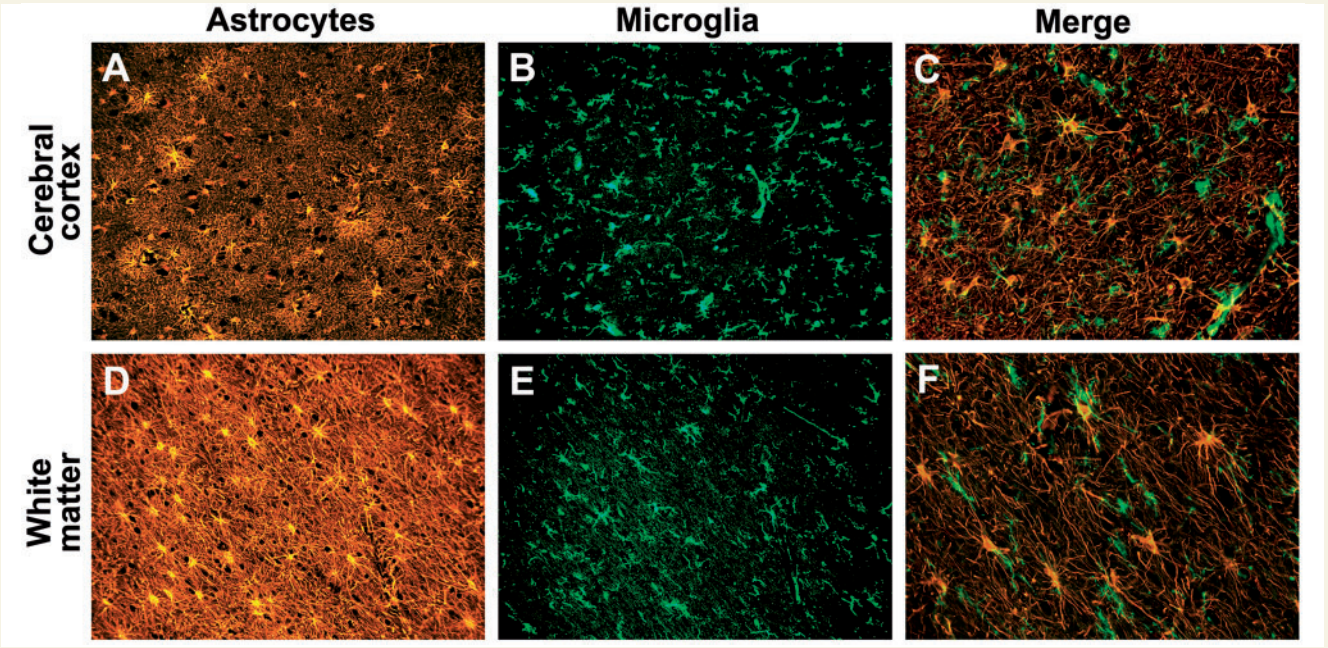

Figure 4 Activated microglia are associated with reactive astrocytosis in sporadic CJD. Reactive astrocytes (anti-GFAP antibody immunostain; orange) and activated microglial cells (anti-IBA1 antibody immunostain; green) in the grey matter (cerebral cortex) and the white matter of the case of CJD that contained a moderate amount of PrP^{Sc} focally in the white matter. (**A**) A moderate degree of reactive astrocytosis in layers 4–5 of cerebral cortex. (**B**) Activated microglia in the same location as **A**, layers 4–5. (**C**) Merge of anti-IBA1 antibody (green) with anti-GFAP antibody (red) in the cortex. (**D**) Severe reactive astrocytic gliosis in the underlying white matter. (**E**) Activated microglia in the white matter in the same region. (**F**) Merge of anti-IBA1 antibody (green) with anti-GFAP antibody (red) white matter showing microglia. In both the grey and white matter, activated microglia appeared intimately associated with reactive astrocytes (**C** and **F**), which however, were not always obviously in contact with activated microglia. This is probably related to the tissue section thickness (8 μm). **A**, **B**, **D** and **E** were taken with a ×20 objective lens; **C** and **F** were taken with a ×40 objective lens. Scale bars: **E** = 100 μm, and also applies to **A**, **B** and **D**; **F** = 100 μm, and also applies to **C**.

compared to controls (Fig. 5). Although, as we previously noted, there was not any statistically significant correlation between histopathological rating scores and mean diffusivity values, the degree of reduced diffusion seen on the attenuation coefficient maps seemed roughly to follow the degree of astrocytic gliosis, but not other pathological changes, present in the tissue (sum of gliosis rating at frontal, parietal, and internal capsule levels) (Fig. 5).

White matter values and clinical scale correlations

There were no significant correlations between clinical scales (modified Barthel, Mini-Mental State Examination and Neuropsychiatric Inventory Scale) and white matter mean diffusivity or fractional anisotropy values, either at a volume of interest or whole brain level ($P > 0.05$).

Discussion

In this study we surprisingly detected widespread white matter involvement in sporadic CJD on diffusion imaging, characterized predominantly by reduced mean diffusivity, with no areas showing increased mean diffusivity. These changes were both in the total white matter as well as regionally within both subcortical and deep white matter. The white matter alteration was clearly visible on the attenuation coefficient map (Fig. 5) and seemed to be associated (although not statistically significant) histopathologically with reactive astrocytic gliosis and activated microglia (Table 3). To our knowledge, this is the first paper to explore the whole brain white matter, and to show global reduced white matter mean diffusivity, in sporadic CJD.

Reduced mean diffusivity in the grey matter (cortical, striatal and/or thalamic) on diffusion-weighted imaging is well-described as highly diagnostic for sporadic CJD (Shiga *et al.*, 2004; Vitali *et al.*, 2011), and most literature suggests a correlation of reduced mean diffusivity with vacuolization and prion deposition, and less so with astrocytic gliosis (Haik *et al.*, 2002; Geschwind *et al.*, 2009; Manners *et al.*, 2009). We now report similarly reduced diffusion in the white matter in sporadic CJD; histopathological findings confirm white matter involvement in sporadic CJD, characterized by pathological alterations partially overlapping with those in sporadic CJD grey matter, but with more diffuse and reactive astrocytic gliosis (and activated microglia) and with rare PrP^{Sc} deposition and vacuolation, present as only microvacuolation (Table 3 and Fig. 3). Pathological vacuolation in the white matter of sporadic CJD can be difficult to differentiate from artefactual

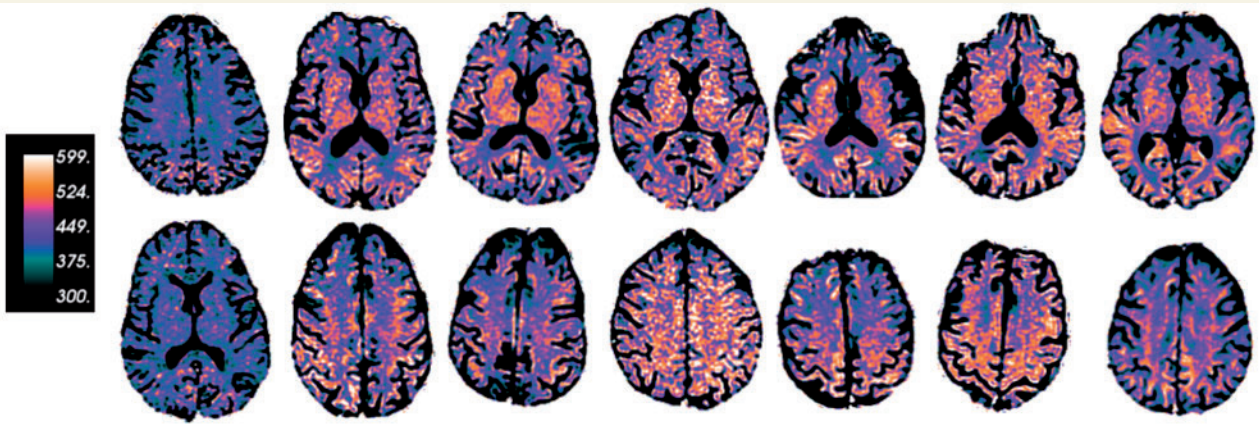

Subjects	Ctrl	sCJD 2	sCJD 5	sCJD 12	sCJD 13	sCJD 18	sCJD 26
Gliosis	-	4	6	6.7	5.75	6.9	3.8

Figure 5 Attenuation coefficient maps of one control and six subjects with sporadic CJD (sCJD) and their histopathological gliosis scores. The attenuation coefficient maps are based on the following formula: exp(−b × mean diffusivity); green/black colours indicate high mean diffusivity and orange/white indicate low mean diffusivity. Note the extensive reduced mean diffusivity in sporadic CJD white matter. To compare the attenuation coefficient maps of each patient to the histopathology rating scores we reported the total gliosis rating based on Table 3. Gliosis total scores were obtained combining frontal, parietal and internal capsule rating scores. Prion deposition and vacuolation are not reported in this figure. Interestingly, there seems to be an association between more reduced mean diffusivity on the attenuation coefficient maps and worse histopathological rating score (Table 3). For example, sCJD subjects 12 and 18, who presented with the worst gliosis scores, had lower mean diffusivity values compared to the other subjects.

vacuolation due to the fixation and staining processes (Garman, 2011). Activated microglia were found throughout the grey matter and white matter and seemed to be intimately associated with reactive astrocytes (Fig. 4C and F). Surprisingly, in all six cases with pathological analysis of the white matter, there were patchy foci of demyelination with no concomitant axonal degeneration.

Although conventional MRI usually do not show any significant white matter involvement in sporadic CJD, animal models of prion disease have described white matter pathology characterized by similar histopathological features to those found in grey matter, with PrP^{Sc} deposition, reactive astrocytes and vacuolation (Taraboulos *et al.*, 1992; Brandner *et al.*, 1996; Prusiner, 1998; Bouzamondo-Bernstein *et al.*, 2004; Safar *et al.*, 2005). Animal models have also suggested a role of normal prion protein (PrP^{C}) in myelin protection/maintenance (Radovanovic *et al.*, 2005; Bremer *et al.*, 2010; Popko, 2010) and a possible role of white matter in the spread of prions in the brain (Kimberlin, 1983; Fraser and Dickinson, 1985; Kordek *et al.*, 1999). Despite this, there are few studies showing evidence of white matter involvement in sporadic CJD (Bugiani *et al.*, 1989; Muhleisen *et al.*, 1995; Armstrong *et al.*, 2002). One study of 15 subjects with CJD examining astrocytosis and vacuolation in the white matter, found diffuse astrocytosis, similar to the grey matter; the vacuolation ranged from subtle microvacuolation to areas with demyelination and severe vacuolation (Bugiani *et al.*, 1989). Another study of six patients with sporadic CJD reported astrocytosis and microglial activation diffusely throughout the white matter, similar to our findings (Muhleisen *et al.*, 1995). Also consistent with our findings, PrP^{Sc} staining did not co-localize with microglia (Muhleisen *et al.*, 1995). Another study examining subcortical white matter pathology in 11 subjects with sporadic CJD found intermittent large clusters of vacuoles accompanied by diffuse astrocytic gliosis. Some of the clusters were distributed with regular periodicity across the base of subcortical white matter, similarly to what they found in the adjacent or overlying grey matter, suggesting to the authors the possibility of cortical-subcortical spread (Armstrong *et al.*, 2002).

We found PrP^{Sc} deposition was overall rare in the white matter, although one case, however, had mild to moderate involvement. This case is consistent with some literature reporting the occasional presence of PrP^{Sc} in the white matter in sporadic CJD (Muhleisen *et al.*, 1995) as well as with mouse models in which PrP^{Sc} is not only routinely detected in the white matter (DeArmond *et al.*, 2002; Spilman *et al.*, 2008), and suggest that it might be transported along white matter axons to distant grey matter regions (Bouzamondo-Bernstein *et al.*, 2004).

In our cases, there were several clear differences between the reactive astrocytosis in the white and grey matter. In the grey matter, the reactive astrocytosis was much less robust and patchier, corroborating previous literature in sporadic CJD and animal models (Syrian hamsters and transgenic mice) in which reactive astrocytosis tended to co-localize with PrP^{Sc}. In the white matter, we found reactive astrocytosis was moderate to severe

and diffuse, but not associated with PrP^{Sc} deposition. What causes these astrocytes to become reactive in CJD is not well understood (Navarro *et al.*, 2004). Interestingly in animal models, PrP^{Sc} seems to induce microglial activation, and this event precedes reactive astrocytosis and neuronal degeneration (Williams *et al.*, 1997; Marella and Chabry, 2004; Liu *et al.*, 2011). In the brain, two major classes of astrocytes, biochemically and developmentally distinct, have been identified on the basis of morphology and distribution in the brain: fibrous astrocytes with many glial filaments composed of GFAP and located mainly in white matter; and protoplasmic astrocytes with few glial filaments and located mainly in grey matter (Miller and Raff, 1984). The different degree of reactive astrocytic gliosis occurring in the white matter compared to grey matter might indicate that protoplasmic astrocytes (in the grey matter) are less capable of forming a dense reactive astrocytic gliosis as fibrous astrocytes (in the white matter). Although the grey matter was filled with deposits of PrP^{Sc}, the white matter in five of six cases showed little or no PrP^{Sc} by immunohistochemistry. The presence of PrP^{Sc} in the grey matter might explain the presence of activated microglia there, however the relative absence or paucity of PrP^{Sc} in the white matter in most of our cases with sporadic CJD raises the question of what causes the microglia to become activated and exuberant reactive astrocytosis to occur in white matter. Furthermore, animal models suggest that PrP^{Sc} is transported between brain regions by axonal transport (Bouzamondo-Bernstein *et al.*, 2004) and that PrP^{Sc} is transported out of neurons by exocytosis to the extracellular space. Perhaps sufficient PrP^{Sc} is exocytosed from axons in the white matter to activate microglia and secondarily cause reactive astrocytosis (DeArmond *et al.*, 1996; Liberski and Budka, 1999; Marella and Chabry, 2004; Bajsarowicz *et al.*, 2012; Kouadir *et al.*, 2012), but the PrP^{Sc} is removed in the process, which is why we do not see it in most cases. The same exocytosis mechanism could result in astrocyte infection with prions and formation of PrP^{Sc} (Raeber *et al.*, 1997). Finally, it is possible that there was sufficient secondary axonal degeneration (although we did not see this by Bielchowsky staining) in the white matter due to neuron loss in the grey matter to account for reactive astrocytic gliosis and activated microglia.

It is peculiar that although our white matter data show a different ratio of histopathological substrates compared to that typically seen in the grey matter, both grey matter and white matter showed reduced mean diffusivity on DTI (Caverzasi *et al.*, 2014) and at the cortical level grey matter and white matter mean diffusivity values correlated quantitatively. Theoretically, vacuolation (Mutsukura *et al.*, 2009), prion deposition, astrocytic gliosis (Geschwind *et al.*, 2009) and/or microgliomatosis could cause reduced mean diffusivity in white matter of sporadic CJD cases (Broom *et al.*, 2007). Although we did not find a statistical correlation between any of these histopathological features and mean diffusivity, this was not unexpected for two reasons. First, the limited amount of data (only six patients and only two regions for each patient) is a limitation of this study and likely negatively affected our ability to discover any statistically significant correlation. Second, we tested a correlation between an averaged mean diffusivity value within an entire Freesurfer volume of interest with histopathological results obtained from a smaller autopsy tissue sample of the same region—the region sampled pathologically might not have been very representative of the larger Freesurfer region averaged for mean diffusivity. Given these limitations, if we have to explain reduced mean diffusivity in white matter based on our histopathological results, it would seem most likely due to astrogliosis and microgliomatosis.

Alternatively, the diffusion changes seen on MRI might not be directly related to histopathology, but could be due to prion disease causing impairment of functional processes in brain cells, such as altered ion channel function due to decreased plasma membrane fluidity (DeArmond *et al.*, 1996) or impaired axonal transport (Liberski and Budka, 1999). Supporting this possibility is that reduced mean diffusivity also occurs during strokes and although the underlying cause of these diffusion changes is still controversial, a membrane dysfunction has been hypothesized (Wardlaw, 2010).

As we found reduced mean diffusivity in white matter of sporadic CJD, our results differ from what it is usually reported in non-prion neurodegenerative diseases, in which white matter damage (whether primary or secondary) usually results in normal to increased mean diffusivity with variability in fractional anisotropy (Pierpaoli *et al.*, 2001; Song *et al.*, 2002; Agosta *et al.*, 2010, 2011; Canu *et al.*, 2011). Surprisingly, our results using DTI and TBSS differ from a study on the TBSS findings in a cohort of patients with genetic CJD with the E200K mutation (Lee *et al.*, 2012), which usually have several clinical and MRI features overlapping with sporadic CJD (Goldfarb *et al.*, 1991; Parchi *et al.*, 1999; Fulbright *et al.*, 2006; Schelzke *et al.*, 2012). In this interesting study on white matter magnetic resonance diffusion in 21 E200K subjects, they found average reduced fractional anisotropy in several white matter tracts (corticospinal tract, internal and external capsule, fornix, and posterior thalamic radiation) mainly due to increased radial diffusivity (with normal axial diffusivity), with a slightly increased mean diffusivity (Lee *et al.*, 2012). In our sporadic CJD cohort we had very different findings. Only a few regions, mostly in frontal and cingulate cortices, showed a significant decrease in fractional anisotropy and, contrary to Lee *et al.* (2012), it was always associated with decreased mean diffusivity. Furthermore, in our study the reduction of fractional anisotropy in these regions was driven by a more substantial reduction of axial diffusivity than radial diffusivity (Supplementary Fig. 1). There are several possible explanations for the different findings. E200K genetic prion disease patients overall have more deep nuclei and less cortical involvement on DWI, than most sporadic CJD cases. The increased radial diffusivity with normal axial diffusivity might be suggestive of demyelination in E200K. Although we are not aware of any CNS demyelination in E200K, demyelination in the PNS has been reported in E200K (Antoine *et al.*, 1996).

Our finding of a greater effect on axial diffusivity (reduction) than radial diffusivity might be due to common neuroaxonal pathological abnormalities in sporadic CJD, such as dystrophic neurites and neurofilament accumulation, which suggests axonal transport abnormalities (Liberski and Budka, 1999) that might lead to primarily reducing axial diffusivity. Another possibility might be that concomitant demyelination, which we found as patchy foci across the white matter regions analysed, leading to a local increase in radial diffusivity (Song *et al.*, 2002), counterbalances some of the reduction of radial diffusivity related to the underlying

cause of the mean diffusivity reduction (e.g. either due to histopathological or functional changes). In the literature, demyelination has been mostly described in CJD mouse models within the peripheral neuronal system (Neufeld *et al.*, 1992; Antoine *et al.*, 1996). To our knowledge, only one previous study, reported in a book chapter, has shown demyelination in the CNS in humans (Bugiani *et al.*, 1989). Although it is not known why CNS demyelination occurs in sporadic CJD, it might be due to leukolysins released by actrocytes and macroglia (Liberski *et al.*, 1989) or to the conversion of the normal prion protein, which appears to be involved in myelin protection/maintenance (Radovanovic *et al.*, 2005; Bremer *et al.*, 2010; Popko, 2010).

Visual assessment

Visual assessment on T_2-weighted images in most subjects did not show any significant white matter changes, except for punctuate deep white matter and thin periventricular white matter abnormalities. A moderate degree of deep white matter T_2 changes, associated with smooth or confluent periventricular and deep white matter foci, were found only in two of 26 subjects. White matter abnormalities on T_2-weighted images were characterized by increased mean diffusivity on attenuation coefficient and mean diffusivity maps (Supplementary Fig. 2) and thus are not the cause of decreased mean diffusivity. Mean diffusivity white matter changes were only appreciable quantitatively, whereas by visual assessment of standard diffusion imaging (DWI and apparent diffusion coefficient map) these abnormalities are usually not detected. We found, however, that attenuation coefficient maps (an inverse of the mean diffusivity maps routinely used), with opposite contrast (Fig. 5) seem to facilitate detection of white matter abnormalities by visual assessment in sporadic CJD. The mild degree of white matter changes detected on visual assessment of T_2 sequences compared to the clear abnormalities on attenuation coefficient, suggests that white matter abnormalities occur on a microstructural level assessed by DTI.

We suggest that the infrequent T_2 abnormalities found on visual assessment in sporadic CJD are likely signs of chronic small vessel disease or, alternatively, initial signs of white matter secondary degeneration. A classic example of white matter secondary degeneration in sporadic CJD is likely represented in the rare panencephalitic form of CJD, reported mostly in Asian countries in which some patients have very long disease durations because the cultures support profound life-extending measures, such as feeding tubes and intubation. In cases with the panencephalitic form of CJD, there is usually significant global atrophy with status spongiosis in grey matter and extensive abnormalities in white matter, correlating with disease duration and severity of cortical atrophy (Mizutani *et al.*, 1981; Carota *et al.*, 1996; Matsusue *et al.*, 2004; Tschampa *et al.*, 2007; Jansen *et al.*, 2009). The panencephalitic form of CJD is probably not so much a specific subtype of CJD, but rather a more non-specific very late, end-stage of exceptionally prolonged cases of CJD, characterized by white matter secondary degeneration to the diffuse late stage neuronal loss (Shyu *et al.*, 1996; Parchi *et al.*, 1999; Iwasaki *et al.*, 2006; Jansen *et al.*, 2009).

Primary versus secondary white matter pathology

In the study of magnetic resonance diffusion in E200K subjects discussed above, the authors speculate about a 'primary' mechanism of white matter damage (a myelinopathy due to the replacement of PrP^C by PrP^{Sc}) leading to a functional disconnection syndrome (Lee *et al.*, 2012), however, histopathological data supporting this hypothesis were not shown.

Our results definitely show white matter abnormalities in sporadic CJD; nevertheless it is challenging to determine whether these white matter changes are primary or secondary. There is some evidence supporting primary involvement of white matter in prion disease. In animal models, PrP^{Sc} appears to induce microglial activation and this event precedes reactive astrocytosis and neuronal degeneration (Marella and Chabry, 2004). Therefore, the widespread restricted diffusion in sporadic CJD white matter in association with reactive astrocytic gliosis and microglial activation (although with rare prion deposition) might represent primary pathogenic events. Due to their cytotoxic potential, astrocytic gliosis and reactive microglial activation might play a major role in sporadic CJD pathogenesis (Liberski *et al.*, 1989; Muhleisen *et al.*, 1995; Marella and Chabry, 2004). In the absence of detectable PrP^{Sc} deposition in the majority of our cases we can only speculate that either a subtle leakage of PrP^{Sc} from axons (Bajsarowicz *et al.*, 2012), or other factors, such as release of interleukins (Marella and Chabry, 2004; Liu *et al.*, 2011; Kouadir *et al.*, 2012), might induce microglia in the white matter. Nevertheless the observation of similar diffusion changes (reduced mean diffusivity) in both white matter and grey matter might indicate that the same primary pathological mechanism is occurring; if so, then reduced mean diffusivity might not be due to specific histopathological changes (e.g. vacuolation, PrP^{Sc} deposition or gliosis), which differed between white matter and grey matter, but rather to some physiological change or dysfunction. At least three findings suggest that the white matter changes (reduced mean diffusivity) identified in our sporadic CJD group are not due to secondary white matter degeneration (caused by neuronal loss). First, as discussed above, our DTI metrics findings were not consistent with axonal degeneration (Pierpaoli *et al.*, 2001; Song *et al.*, 2002; Agosta *et al.*, 2010, 2011; Canu *et al.*, 2011); second, there was not significant grey matter atrophy in our cohort (Caverzasi *et al.*, 2014); and third, there was no evidence for axonal white matter degeneration on histopathology.

In conclusion, this work shows for the first time a widespread reduced mean diffusivity within the white matter of subjects with sporadic CJD. This imaging finding may provide an additional imaging feature that could be used in the differential diagnosis of CJD, although this needs to be assessed. Our histopathological analyses showed concomitant astrocytic gliosis and microglial activation, with patchy foci of demyelination; although these changes were not statistically correlated with reduced mean diffusivity, this might have been due to insufficient power. We did not find axonal degeneration, which is generally associated with increased mean diffusivity. These imaging and histopathological findings may reflect direct white matter damages occurring

during early to middle stages of sporadic CJD, rather than changes secondary to neuronal degeneration/loss.

Funding

Dr S.J. DeArmond was funded by NIH (AG021601); Dr Geschwind was funded by NIH/NIA R01 AG-031189, NIH/NIA K23 AG021989; NIH/NIA AG031220 and Michael J. Homer Family Fund.

Supplementary material

Supplementary material is available at *Brain* online.

References

Agosta F, Pagani E, Petrolini M, Caputo D, Perini M, Prelle A, et al. Assessment of white matter tract damage in patients with amyotrophic lateral sclerosis: a diffusion tensor MR imaging tractography study. AJNR Am J Neuroradiol 2010; 31: 1457–61.

Agosta F, Pievani M, Sala S, Geroldi C, Galluzzi S, Frisoni GB, et al. White matter damage in Alzheimer disease and its relationship to gray matter atrophy. Radiology 2011; 258: 853–63.

Antoine JC, Laplanche JL, Mosnier JF, Beaudry P, Chatelain J, Michel D. Demyelinating peripheral neuropathy with Creutzfeldt-Jakob disease and mutation at codon 200 of the prion protein gene. Neurology 1996; 46: 1123–7.

Armstrong RA, Lantos PL, Cairns NJ. Spatial patterns of the vacuolation in subcortical white matter in sporadic Creutzfeldt-Jakob disease (sCJD). Clin Neuropathol 2002; 21: 284–8.

Bajsarowicz K, Ahn M, Ackerman L, Dearmond BN, Carlson G, DeArmond SJ. A brain aggregate model gives new insights into the pathobiology and treatment of prion diseases. J Neuropathol Exp Neurol 2012; 71: 449–66.

Bouzamondo-Bernstein E, Hopkins SD, Spilman P, Uyehara-Lock J, Deering C, Safar J, et al. The neurodegeneration sequence in prion diseases: evidence from functional, morphological and ultrastructural studies of the GABAergic system. J Neuropathol Exp Neurol 2004; 63: 882–99.

Brandner S, Raeber A, Sailer A, Blattler T, Fischer M, Weissmann C, et al. Normal host prion protein (PrP^{C}) is required for scrapie spread within the central nervous system. Proc Natl Acad Sci USA 1996; 93: 13148–51.

Bremer J, Baumann F, Tiberi C, Wessig C, Fischer H, Schwarz P, et al. Axonal prion protein is required for peripheral myelin maintenance. Nat Neurosci 2010; 13: 310–8.

Broom KA, Anthony DC, Lowe JP, Griffin JL, Scott H, Blamire AM, et al. MRI and MRS alterations in the preclinical phase of murine prion disease: association with neuropathological and behavioural changes. Neurobiol Dis 2007; 26: 707–17.

Brown P, Cathala F, Castaigne P, Gajdusek DC. Creutzfeldt-Jakob disease: clinical analysis of a consecutive series of 230 neuropathologically verified cases. Ann Neurol 1986; 20: 597–602.

Bugiani O, Tagliavini F, Giaccone G, Boeri R. Chapter 6. Creutzfeldt-Jakob disease: astrocytosis and spongiform changes of the white matter. In: Court LA, Dormont D, Brown P, Kingsbury DT, editors. Unconventional virus diseases of the central nervous system. Paris: Commisariat à l'Energie Atomique; 1989. p. 172–83.

Canu E, Agosta F, Riva N, Sala S, Prelle A, Caputo D, et al. The topography of brain microstructural damage in amyotrophic lateral sclerosis assessed using diffusion tensor MR imaging. AJNR Am J Neuroradiol 2011; 32: 1307–14.

Carota A, Pizzolato GP, Gailloud P, Macchi G, Fasel J, Le Floch J, et al. A panencephalopathic type of Creutzfeldt-Jakob disease with selective lesions of the thalamic nuclei in 2 Swiss patients. Clin Neuropathol 1996; 15: 125–34.

Caverzasi E, Henry RG, Vitali P, Lobach IV, Kornak J, Bastianello S, et al. Application of quantitative DTI metrics in sporadic CJD. Neuroimage Clin 2014; 4: 426–35.

Cummings JL. The Neuropsychiatric Inventory: assessing psychopathology in dementia patients. Neurology 1997; 48: S10–S16.

Dale AM, Fischl B, Sereno MI. Cortical surface-based analysis. I. Segmentation and surface reconstruction. Neuroimage 1999; 9: 179–94.

DeArmond SJ, Kretzschmar HA, Prusiner SB. Prion diseases. In: Graham DI, Lantos PL, editors. Greenfield's neuropathology. 7th edn. New York: Arnold; 2002. p. 273–323.

DeArmond SJ, Qiu Y, Wong K, Nixon R, Hyun W, Prusiner SB, et al. Abnormal plasma membrane properties and functions in prion-infected cell lines. Cold Spring Harb Symp Quant Biol 1996; 61: 531–40.

Deguchi K, Takamiya M, Deguchi S, Morimoto N, Kurata T, Ikeda Y, et al. Spreading brain lesions in a familial Creutzfeldt-Jakob disease with V180I mutation over 4 years. BMC Neurol 2012; 12: 144.

Demaerel P, Heiner L, Robberecht W, Sciot R, Wilms G. Diffusion-weighted MRI in sporadic Creutzfeldt-Jakob disease. Neurology 1999; 52: 205–8.

Fischl B, Sereno MI, Dale AM. Cortical surface-based analysis. II: inflation, flattening, and a surface-based coordinate system. Neuroimage 1999; 9: 195–207.

Fraser H, Dickinson AG. Targeting of scrapie lesions and spread of agent via the retino-tectal projection. Brain Res 1985; 346: 32–41.

Fulbright RK, Kingsley PB, Guo X, Hoffmann C, Kahana E, Chapman JC, et al. The imaging appearance of Creutzfeldt-Jakob disease caused by the E200K mutation. Magn Reson Imaging 2006; 24: 1121–9.

Galanaud D, Haik S, Linguraru MG, Ranjeva JP, Faucheux B, Kaphan E, et al. Combined diffusion imaging and MR spectroscopy in the diagnosis of human prion diseases. AJNR Am J Neuroradiol 2010; 31: 1311–8.

Garman RH. Histology of the central nervous system. Toxic Path 2011; 39: 22–35.

Geschwind MD, Haman A, Miller BL. Rapidly progressive dementia. Neurol Clin 2007; 25: 783–807.

Geschwind MD, Potter CA, Sattavat M, Garcia PA, Rosen HJ, Miller BL, et al. Correlating DWI MRI with pathologic and other features of Jakob-Creutzfeldt disease. Alzheimer Dis Assoc Disord 2009; 23: 82–7.

Ghorayeb I, Series C, Parchi P, Sawan B, Guez S, Laplanche JL, et al. Creutzfeldt-Jakob disease with long duration and panencephalopathic lesions: molecular analysis of one case. Neurology 1998; 51: 271–4.

Goldfarb LG, Brown P, Mitrova E, Cervenakova L, Goldin L, Korczyn AD, et al. Creutzfeldt-Jacob disease associated with the PRNP codon 200Lys mutation: an analysis of 45 families. Eur J Epidemiol 1991; 7: 477–86.

Haik S, Dormont D, Faucheux BA, Marsault C, Hauw JJ. Prion protein deposits match magnetic resonance imaging signal abnormalities in Creutzfeldt-Jakob disease. Ann Neurol 2002; 51: 797–9.

Hama T, Iwasaki Y, Niwa H, Yoshida M, Hashizume Y, Kitamoto T, et al. An autopsied case of panencephalopathic-type Creutzfeldt-Jakob disease with mutation in the prion protein gene at codon 232 and type 1 prion protein. Neuropathology 2009; 29: 727–34.

Iwasaki Y, Yoshida M, Hashizume Y, Kitamoto T, Sobue G. Clinicopathologic characteristics of sporadic Japanese Creutzfeldt-Jakob disease classified according to prion protein gene polymorphism and prion protein type. Acta Neuropathol 2006; 112: 561–71.

Jansen C, Head MW, Rozemuller AJ, Ironside JW. Panencephalopathic Creutzfeldt-Jakob disease in the Netherlands and the UK: clinical and pathological characteristics of nine patients. Neuropathol Appl Neurobiol 2009; 35: 272–82.

Kanazawa H, Ohsawa K, Sasaki Y, Kohsaka S, Imai Y. Macrophage/microglia-specific protein Iba1 enhances membrane ruffling and Rac activation via phospholipase C-gamma -dependent pathway. J Biol Chem 2002; 277: 20026–32.

Kimberlin RH, Walker Carol A. The antiviral compound HPA-23 can prevent scrapie when administered at the time of infection. Arch Virol 1983; 78: 9–18.

Kordek R, Hainfellner JA, Liberski PP, Budka H. Deposition of the prion protein (PrP) during the evolution of experimental Creutzfeldt-Jakob disease. Acta Neuropathol 1999; 98: 597–602.

Kouadir M, Yang L, Tan R, Shi F, Lu Y, Zhang S, et al. CD36 participates in PrP(106-126)-induced activation of microglia. PLoS One 2012; 7: e30756.

Kretzschmar HA, Ironside JW, DeArmond SJ, Tateishi J. Diagnostic criteria for sporadic Creutzfeldt-Jakob disease. Arch Neurol 1996; 53: 913–20.

Kruger H, Meesmann C, Rohrbach E, Muller J, Mertens HG. Panencephalopathic type of Creutzfeldt-Jakob disease with primary extensive involvement of white matter. Eur Neurol 1990; 30: 115–9.

Kucharczyk W, Bergeron C. Primary white matter involvement in sporadic-type Creutzfeldt-Jakob disease? Which came first, the chicken or the egg? AJNR Am J Neuroradiol 2004; 25: 905–6.

Lee H, Cohen OS, Rosenmann H, Hoffmann C, Kingsley PB, Korczyn AD, et al. Cerebral white matter disruption in Creutzfeldt-Jakob disease. AJNR Am J Neuroradiol 2012; 33: 1945–50.

Liberski PP, Budka H. Neuroaxonal pathology in Creutzfeldt-Jakob disease. Acta Neuropathol 1999; 97: 329–34.

Liberski PP, Yanagihara R, Gibbs CJ Jr., Gajdusek DC. White matter ultrastructural pathology of experimental Creutzfeldt-Jakob disease in mice. Acta Neuropathol 1989; 79: 1–9.

Liu W, Tang Y, Feng J. Cross talk between activation of microglia and astrocytes in pathological conditions in the central nervous system. Life Sci 2011; 89: 141–6.

Mahoney F, Barthel D. Functional evaluation: Barthel Index. Md State Med J 1965; 14: 61–5.

Manners DN, Parchi P, Tonon C, Capellari S, Strammiello R, Testa C, et al. Pathologic correlates of diffusion MRI changes in Creutzfeldt-Jakob disease. Neurology 2009; 72: 1425–31.

Marella M, Chabry J. Neurons and astrocytes respond to prion infection by inducing microglia recruitment. J Neurosci 2004; 24: 620–7.

Matsusue E, Kinoshita T, Sugihara S, Fujii S, Ogawa T, Ohama E. White matter lesions in panencephalopathic type of Creutzfeldt-Jakob disease: MR imaging and pathologic correlations. AJNR Am J Neuroradiol 2004; 25: 910–8.

Meissner B, Kallenberg K, Sanchez-Juan P, Collie D, Summers DM, Almonti S, et al. MRI lesion profiles in sporadic Creutzfeldt-Jakob disease. Neurology 2009; 72: 1994–2001.

Miller RH, Raff MC. Fibrous and protoplasmic astrocytes are biochemically and developmentally distinct. J Neurosci 1984; 4: 585–92.

Mizutani T, Okumura A, Oda M, Shiraki H. Panencephalopathic type of Creutzfeldt-Jakob disease: primary involvement of the cerebral white matter. J Neurol Neurosurg Psychiatry 1981; 44: 103–15.

Muhleisen H, Gehrmann J, Meyermann R. Reactive microglia in Creutzfeldt-Jakob disease. Neuropathol Appl Neurobiol 1995; 21: 505–17.

Mutsukura K, Satoh K, Shirabe S, Tomita I, Fukutome T, Morikawa M, et al. Familial Creutzfeldt-Jakob disease with a V180I mutation: comparative analysis with pathological findings and diffusion-weighted images. Dement Geriatr Cogn Disord 2009; 28: 550–7.

Navarro A, Del Valle E, Tolivia J. Differential expression of apolipoprotein D in human astroglial and oligodendroglial cells. J Histochem Cytochem 2004; 52: 1031–6.

Neufeld MY, Josiphov J, Korczyn AD. Demyelinating peripheral neuropathy in Creutzfeldt-Jakob disease. Muscle Nerve 1992; 15: 1234–9.

Pantoni L, Simoni M, Pracucci G, Schmidt R, Barkhof F, Inzitari D. Visual rating scales for age-related white matter changes (leukoaraiosis): can the heterogeneity be reduced? Stroke 2002; 33: 2827–33.

Parchi P, Giese A, Capellari S, Brown P, Schulz-Schaeffer W, Windl O, et al. Classification of sporadic Creutzfeldt-Jakob disease based on molecular and phenotypic analysis of 300 subjects. Ann Neurol 1999; 46: 224–33.

Pierpaoli C, Barnett A, Pajevic S, Chen R, Penix LR, Virta A, et al. Water diffusion changes in Wallerian degeneration and their dependence on white matter architecture. Neuroimage 2001; 13: 1174–85.

Popko B. Myelin maintenance: axonal support required. Nat Neurosci 2010; 13: 275–7.

Prusiner SB. Prions. Proc Natl Acad Sci USA 1998; 95: 13363–83.

Radovanovic I, Braun N, Giger OT, Mertz K, Miele G, Prinz M, et al. Truncated prion protein and Doppel are myelinotoxic in the absence of oligodendrocytic PrP^{C}. J Neurosci 2005; 25: 4879–88.

Raeber AJ, Race RE, Brandner S, Priola SA, Sailer A, Bessen RA, et al. Astrocyte-specific expression of hamster prion protein (PrP) renders PrP knockout mice susceptible to hamster scrapie. EMBO J 1997; 16: 6057–65.

Safar JG, Geschwind MD, Deering C, Didorenko S, Sattavat M, Sanchez H, et al. Diagnosis of human prion disease. Proc Natl Acad Sci USA 2005; 102: 3501–6.

Satoh K, Shirabe S, Tsujino A, Eguchi H, Motomura M, Honda H, et al. Total tau protein in cerebrospinal fluid and diffusion-weighted MRI as an early diagnostic marker for Creutzfeldt-Jakob disease. Dement Geriatr Cogn Disord 2007; 24: 207–12.

Scheltens P, Barkhof F, Leys D, Pruvo JP, Nauta JJ, Vermersch P, et al. A semiquantative rating scale for the assessment of signal hyperintensities on magnetic resonance imaging. J Neurol Sci 1993; 114: 7–12.

Schelzke G, Kretzschmar HA, Zerr I. Clinical aspects of common genetic Creutzfeldt-Jakob disease. Eur J Epidemiol 2012; 27: 147–9.

Shiga Y, Miyazawa K, Sato S, Fukushima RS, Shibuya S, Sato Y, et al. Diffusion-weighted MRI abnormalities as an early diagnostic marker for Creutzfeldt-Jakob disease. Neurology 2004; 63: 443–9.

Shyu WC, Hsu YD, Kao MC, Tsao WL. Panencephalitic Creutzfeldt-Jakob disease in a Chinese family. Unusual presentation with PrP codon 210 mutation and identification by PCR-SSCP. J Neurol Sci 1996; 143: 176–80.

Smith SM, Jenkinson M, Johansen-Berg H, Rueckert D, Nichols TE, Mackay CE, et al. Tract-based spatial statistics: voxelwise analysis of multi-subject diffusion data. Neuroimage 2006; 31: 1487–505.

Song SK, Sun SW, Ramsbottom MJ, Chang C, Russell J, Cross AH. Dysmyelination revealed through MRI as increased radial (but unchanged axial) diffusion of water. Neuroimage 2002; 17: 1429–36.

Spilman P, Lessard P, Sattavat M, Bush C, Tousseyn T, Huang EJ, et al. A gamma-secretase inhibitor and quinacrine reduce prions and prevent dendritic degeneration in murine brains. Proc Natl Acad Sci USA 2008; 105: 10595–600.

Taraboulos A, Jendroska K, Serban D, Yang SL, DeArmond SJ, Prusiner SB. Regional mapping of prion proteins in brain. Proc Natl Acad Sci USA 1992; 89: 7620–4.

Tschampa HJ, Kallenberg K, Kretzschmar HA, Meissner B, Knauth M, Urbach H, et al. Pattern of cortical changes in sporadic Creutzfeldt-Jakob disease. AJNR Am J Neuroradiol 2007; 28: 1114–8.

Vitali P, Maccagnano E, Caverzasi E, Henry RG, Haman A, Torres-Chae C, et al. Diffusion-weighted MRI hyperintensity patterns differentiate CJD from other rapid dementias. Neurology 2011; 76: 1711–9.

Wang LH, Bucelli RC, Patrick E, Rajderkar D, Alvarez Iii E, Lim MM, et al. Role of magnetic resonance imaging, cerebrospinal fluid, and electroencephalogram in diagnosis of sporadic Creutzfeldt-Jakob disease. J Neurol 2013; 260: 498–506.

Wardlaw JM. Neuroimaging in acute ischaemic stroke: insights into unanswered questions of pathophysiology. J Intern Med 2010; 267: 172–90.

Williams A, Lucassen PJ, Ritchie D, Bruce M. PrP deposition, microglial activation, and neuronal apoptosis in murine scrapie. Exp Neurol 1997; 144: 433–8.

Yamada M, Itoh Y, Suematsu N, Matsushita M, Otomo E. Panencephalopathic type of Creutzfeldt-Jakob disease associated with cadaveric dura mater graft. J Neurol Neurosurg Psychiatry 1997; 63: 524–7.

Young GS, Geschwind MD, Fischbein NJ, Martindale JL, Henry RG, Liu S, et al. Diffusion-weighted and fluid-attenuated inversion recovery imaging in Creutzfeldt-Jakob disease: high sensitivity and specificity for diagnosis. AJNR Am J Neuroradiol 2005; 26: 1551–62.

Zerr I, Kallenberg K, Summers DM, Romero C, Taratuto A, Heinemann U, et al. Updated clinical diagnostic criteria for sporadic Creutzfeldt-Jakob disease. Brain 2009; 132: 2659–68.